

See discussions, stats, and author profiles for this publication at: <https://www.researchgate.net/publication/269998813>

# Effect of molecular weight on conformational changes of PEO: an infrared spectroscopic analysis

ARTICLE *in* JOURNAL OF MATERIALS SCIENCE · FEBRUARY 2015

Impact Factor: 2.37 · DOI: 10.1007/s10853-014-8714-1

---

READS

36

4 AUTHORS, INCLUDING:



Shuyan Yang

Dongguan University of Technology

9 PUBLICATIONS 33 CITATIONS

SEE PROFILE



Yuanqi Jiao

Dongguan University of Technology

4 PUBLICATIONS 6 CITATIONS

SEE PROFILE

# Effect of molecular weight on conformational changes of PEO: an infrared spectroscopic analysis

Shuyan Yang · Zhimeng Liu · Yuping Liu · Yuanqi Jiao

Received: 22 August 2014 / Accepted: 8 November 2014 / Published online: 21 November 2014  
© Springer Science+Business Media New York 2014

**Abstract** Effect of molecular weight on conformation, helix structure (H structure) and trans planar structure (T structure), of Poly(ethylene oxide) (PEO) has been investigated in detail by X-ray diffraction (XRD), Fourier transform infrared spectroscopy (FTIR), and differential scanning calorimeter. Two main diffraction peaks at about  $2\theta = 19^\circ$  and  $23^\circ$  are discovered, and XRD patterns reveal that the unit cell of crystalline PEO belongs to the monoclinic lattice. The crystallinity decreases from 93.82 to 59.62 %, and the deviation of crystalline temperature of PEO-0.5 is larger than those of the other three under four reheated cycles. From FTIR results, a red shift about  $11\text{ cm}^{-1}$  is observed in the stretching vibration of  $-\text{C}-\text{O}-\text{C}-$  with increasing molecular weight, suggesting the presence of chain–chain interactions to restrict the stretching vibration of  $-\text{C}-\text{O}-\text{C}-$  in main chains. Meanwhile, the bending region of  $-\text{C}-\text{C}-\text{O}-$  at about  $533\text{ cm}^{-1}$  sensitive to tension shifts to lower wavenumber, and a new peak at about  $510\text{ cm}^{-1}$  emerges with increasing molecular weight, which is the indicator of internal tension/strain and orientation. Furthermore, the peak intensity ratios of H structure decrease with increasing molecular weight. In contrast, T structure increases dramatically. Consequently, with respect to molecular weight, the possible interactions, entanglements and tie molecules, of PEO molecular chains to explain the difference between H and T structure is

proposed, which is in agreement with the experimental observations quite well.

## Introduction

Polymer crystallization is one of the most intriguing topics in macromolecule science and even condensed matter physics. It is universally acknowledged that most of the biodegradable polymers are semicrystalline, and their applications are dominated by materials properties (such as material chemical structure and aggregation structure [1]), which is molecular weight-dependent partially [2]. Thereby, it is significant importance to understand the crystalline morphology and molecular packing structure of polymers. Poly(ethylene oxide) (PEO) is a semicrystalline polymer with tremendous applications, such as drug release [3] and solid state polymer electrolytes [4, 5]. The diffusivity of the drug through the matrix, the swelling of the polymer, and its solubilization rate can be biased by changing the molecular weight of the polymer or blending polymer fractions with different molecular weights [3]. Moreover, the crystallinity and molecular configuration (helix or trans planar zigzag) of PEO greatly influence its properties and application, especially in lithium-battery field. In our preview works, the crystalline behavior and morphology of PEO are affected by molecular interactions [1] and nano-confinement within nanotubes [6] significantly. It has been found that in the polymer electrolytes, the ionic transport through the amorphous phase of semicrystalline polymers is several orders of magnitude higher than that in the crystalline phase. However, experiments from Bruce et al. showed that crystalline polymer electrolytes based on PEO not only conducted but also did so better than the analogous amorphous phases [7]. Further

S. Yang · Z. Liu (✉) · Y. Liu · Y. Jiao  
Chemical Industrial Cleaner Production and Green Chemical  
R&D Center of Guang Dong Universities, Dongguan University  
of Technology, Dongguan 523808, People's Republic of China  
e-mail: zmliu1234@126.com

S. Yang · Z. Liu · Y. Liu · Y. Jiao  
Dongguan Cleaner Production Center, Dongguan 523808,  
People's Republic of China

investigations suggested that the highest ionic conductivity was originated from the formation of helix crystal structure [5]. Bruce assigned this high ionic conductivity to the vacancies available for cation transport that facilitated a conduction mechanism involving cooperative displacement of lithium ions along the cylindrical tunnels (helix crystal structure) [8]. Still, to our knowledge, it is unknown that how the molecular weight affects the molecular conformation of PEO.

In this work, four PEO samples with different number average molecular weights were acquired to reveal the effect of molecular weight on the crystal and molecular conformation of PEO. X-ray diffraction (XRD) and differential scanning calorimeter (DSC) were applied to investigate the crystal behavior of PEO. Finally, the molecular conformation of PEO with different molecular weights was uncovered by Fourier transform infrared spectroscopy (FTIR) analysis.

## Experimental section

### Materials and preparation

Four PEO samples, from Sigma-Aldrich, were used without further purification, and the number average molecular weights were  $5.0 \times 10^3$  (PEO-0.5),  $1.0 \times 10^5$  (PEO-10),  $1.0 \times 10^6$  (PEO-100), and  $4.0 \times 10^6$  (PEO-400), respectively.

0.5 g PEO powders were dissolved in 6 ml acetonitrile with vigorous stir for 3 h and then were poured into a Teflon home-made model. The models were moved into a fume cupboard for solvent evaporation under atmosphere, and then the PEO membranes were achieved by evaporating the residual solvents in a vacuum oven at 40 °C for 24 h until the samples kept constant.

## Characterization

### X-Ray diffraction analysis

XRD measurements of PEO membranes were performed on an Ultima IV multipurpose XRD system using 44 mA current and 40 kV, with Cu  $K_\alpha$  radiation ( $\lambda = 0.1542$  nm). The membranes were scanned in a continuous mode from 10° to 35° at a step width of 0.02°.

### FTIR measurements of PEO membranes

The FTIR analysis was conducted by a Bruker Tensor 27 spectrometer. Spectra were taken from 400 to 4000  $\text{cm}^{-1}$  with resolving power of 2  $\text{cm}^{-1}$ .

## DSC measurement

Before testing, all the prepared samples were kept at a constant temperature of 40 °C for 12 h. Then the crystalline behaviors of PEO membranes were carried out at a heating rate of 10 °C/min from 20 to 100 °C and then were kept at 100 °C for 10 min, following by a cooling incident from 100 to −20 °C (kept for 10 min) at the cooling rate of −10 °C/min. After that, another rising temperature to 100 °C with the heating rate of 10 °C/min was carried out. The heating/cooling incidents were repeated four times, as shown in Fig. 1. The crystallinity of PEO membranes was calculated from cooling processes of DSC curves according to Ref. [1].

## Results and discussion

### XRD analysis of PEO membranes

The XRD patterns of PEO membranes with different molecular weights are shown in Fig. 2, from which it is obvious that the peak positions of PEO are almost identical, indicating that PEO chains form a similar crystal structure although the molecular weight is different from each other. In Fig. 2, the peak positions of the four samples are in accordance with those from ref [9], which can be deduced that a monoclinic crystal structure is introduced in the crystalline PEO [10]. In order to clearly understand the unit-cell structure parameters of PEO crystals, the precise values of peak positions can be obtained from Fig. 2. For a monoclinic system, the inter-planar spacing of the (hkl) reflection planes is given by

$$\left(\frac{1}{d_{hkl}}\right)^2 = \left(\frac{2 \sin(\theta_{hkl}/2)}{\lambda}\right)^2 = \frac{1}{\sin^2 \beta} \left( \frac{h^2}{a^2} + \frac{k^2 \sin^2 \beta}{b^2} + \frac{l^2}{c^2} - \frac{2hl \cos \beta}{ac} \right) \quad (1)$$

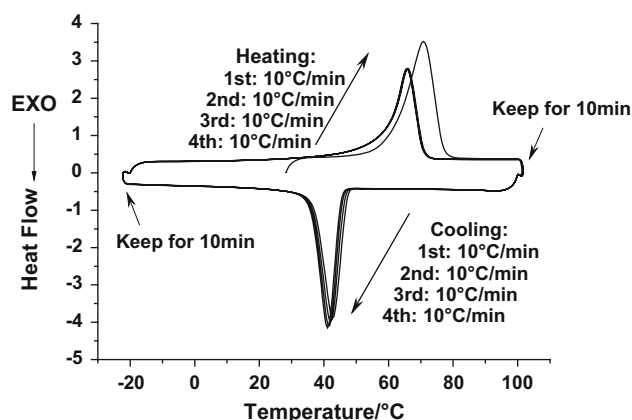
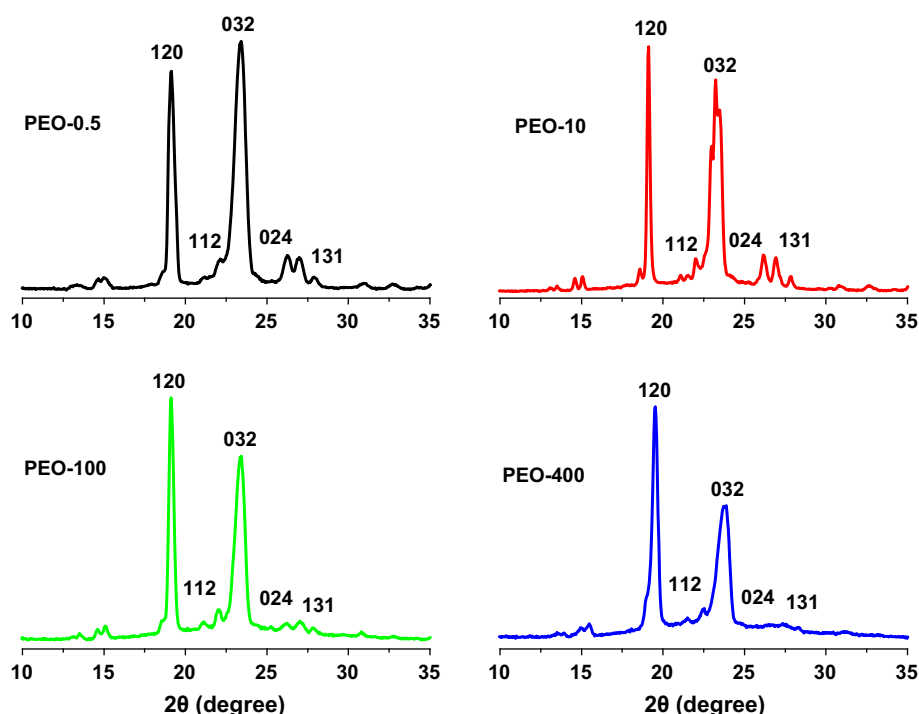


Fig. 1 The schematic diagram of DSC curves for four cycles

**Fig. 2** XRD profiles of PEO with different molecular weights



**Table 1** Unit-Cell structure and crystalline parameters of PEO crystals with different number average molecular weights

Sample	PEO-0.5	PEO-10	PEO-100	PEO-400
a (Å)	8.09	8.01	8.19	7.98
b (Å)	12.98	13.10	12.96	12.76
c (Å)	19.50	19.56	19.55	19.49

Here, the value of  $\beta$  is  $125.4^\circ$  for PEO [10]. By the insertion of the values of  $\lambda = 1.542 \text{ \AA}$  and the any three  $\theta$  values of reflection planes (120), (032), (131), (024), and (112), monoclinic crystal structure parameters  $a$ ,  $b$ , and  $c$  of PEO membranes are determined by Eq. (1) and listed in Table 1 as the dependence of molecular weight. From Table 1, one can see that the monoclinic crystal structure parameters  $a$ ,  $b$ , and  $c$  remain almost the same without respect to the molecular weight. That is, without external applied tension or molecular segments tension [11], PEO molecules tend to form monoclinic crystal structure, which is in accordance with other researchers' works [10, 12]. Two main reasons may be responsible for this phenomenon [11]: First, two or more PEO crystal fragments often form at different sites [2] and are connected by loose domain due to the less perfect crystal of pure PEO single crystals. The monoclinic structure of PEO prefers to form twins and multi-twins, leading to a lower packing energy of molecular segments. Second, the motion of molecular segments in the monoclinic structure seems to be more active, resulting in chain segments rearrangement readily.

#### FTIR analysis of PEO

Infrared spectroscopy is a sensitive and powerful tool to study changes of dipole moments in chemical groups caused by chemical or physical interactions, and it also provides information on crystallinity in terms of the split of single peak [1, 4] and on changes of peak position, width, and intensity [6, 9]. The FTIR traces of PEO with different molecular weights are shown in Fig. 3, and for clearly understanding the evolutions in  $-\text{CH}_2-$  and  $-\text{C}-\text{O}-\text{C}-$  groups vibration of PEO, the characteristic positions of these groups are illuminated in Table 2 detailedly. The most dominant absorptions in the range of  $4000\text{--}400 \text{ cm}^{-1}$  are two absorption regions: One locates between  $3000$  and  $2700 \text{ cm}^{-1}$  originating from methylene stretching, and the other complex in the region from  $1500$  to  $750 \text{ cm}^{-1}$  results from the combination of ether group stretching and methylene group wagging/twisting/rocking modes. The band occurring around  $2884 \text{ cm}^{-1}$  corresponds to the C–H symmetric stretching vibration of  $-\text{CH}_2-$ , which moves to higher wavenumber, i.e., a blue shift about  $5 \text{ cm}^{-1}$ , with increasing the molecular weight, indicating that the circumstance of  $-\text{CH}_2-$  in PEO films may be different. This is also suitable for the twisting ( $1234 \text{ cm}^{-1}$ ) and rocking ( $960 \text{ cm}^{-1}$ ) vibrations of  $-\text{CH}_2-$  that a blue shift is observed. Three  $-\text{C}-\text{O}-\text{C}-$  peaks appear at  $1145$ ,  $1116$ , and  $1062 \text{ cm}^{-1}$ , which is indicator of crystallinity of PEO [1, 6]. Although the absorption intensity at the  $1116 \text{ cm}^{-1}$  is the strongest, all others are of medium, and the absorption

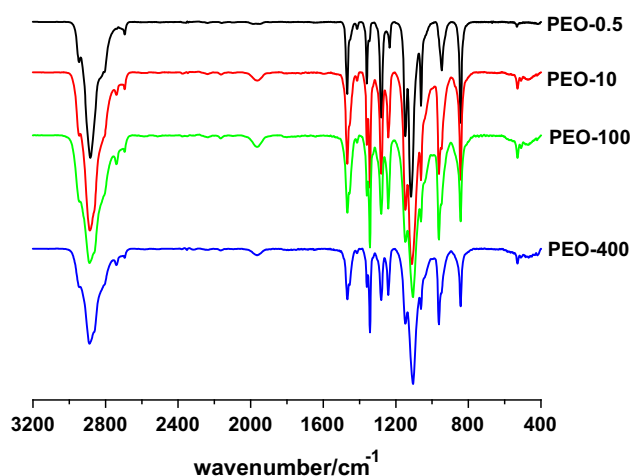


**Fig. 3** The whole FTIR profiles of PEO with different molecular weights

at  $1145\text{ cm}^{-1}$  is somewhat stronger than that at  $1062\text{ cm}^{-1}$ . The changes in peak positions are informative. To our interest, one can see that a red shift about  $11\text{ cm}^{-1}$  is obtained in the strongest peak  $\text{-C-O-C-}$  at  $1116\text{ cm}^{-1}$  with increasing molecular weight, suggesting that some interactions, like chain–chain interactions [13], may be introduced to restrain stretching vibration of  $\text{-C-O-C-}$  in the main chain. In this case, a network may be formed by physical entanglements [14].

It is well known that some bands in the FTIR spectrum are strongly dependent on the conformation of molecules. Recently, by casting a film of PEO from solution at room temperature, an unquestionable experimental result is that the FTIR spectrum of PEO shows a multiplicity of  $\text{-CH}_2\text{-}$  vibration modes, which is an experimental proof that at least two kinds of PEO with different molecular conformations coexist in the as-casting film. These conformations are known as the helical structure (noted as H) and trans planar structure (noted as T) for PEO films [9, 11, 12]. The band

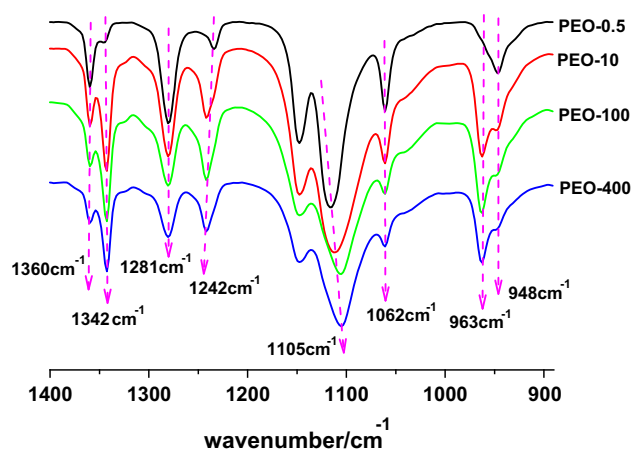


**Fig. 4** FTIR spectra in absorbance scales of  $1400\text{--}900\text{ cm}^{-1}$  for PEO films with different molecular weights

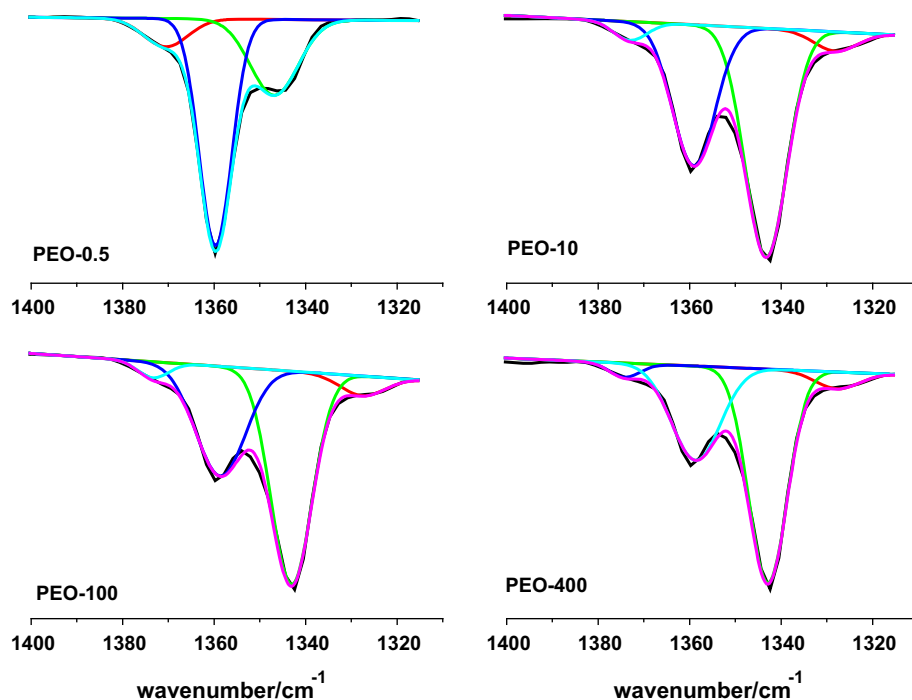
occurring at  $1360/1343$ ,  $1281/1242$ , and  $962/948/843\text{ cm}^{-1}$  is attributed to the asymmetric wagging mode, asymmetric twisting mode, and symmetric rocking mode of  $\text{-CH}_2\text{-}$ , respectively [15, 16]. It is universally acknowledged that the frequency, width, and intensity of these  $\text{-CH}_2\text{-}$  vibrations are very sensitive to the intermolecular interactions, the variation of macromolecular conformations, and the crystalline structures of PEO [17]. The most characteristic bands of H structure are  $1360$  ( $\text{-CH}_2\text{-}$  wagging),  $1281$  ( $\text{-CH}_2\text{-}$  twisting),  $948$ , and  $843\text{ cm}^{-1}$  ( $\text{-CH}_2\text{-}$  rocking), and those of T structure are at  $1343$  ( $\text{-CH}_2\text{-}$  wagging),  $1242$  ( $\text{-CH}_2\text{-}$  twisting), and  $962\text{ cm}^{-1}$  ( $\text{-CH}_2\text{-}$  rocking) [9, 13]. For distinctly understanding differences among these characteristic bands, a magnification of the bands in the range of  $1400\text{--}900\text{ cm}^{-1}$  is shown in Fig. 4 thoroughly. The most important information in Fig. 4 is the changes of peak intensities. However, it is widely believed that the peak intensity is closed relative to the thickness of film when measuring. As a consequence, some reports suggested taking the peak intensity of

**Table 2** Characteristic peaks and peaks intensity ratios  $I_x/I_{1467}^a$  for PEO samples

Sample	PEO-0.5	PEO-10	PEO-100	PEO-400
$\nu_s(\text{CH}_2)$	2884	2886	2888	2889
$w(\text{CH}_2)$	1360, 1347	1359, 1343	1359, 1343	1359, 1343
$\beta(\text{CH}_2)$	1467	1467	1467	1467
$t(\text{CH}_2)$	1281, 1234	1281, 1242	1281, 1242	1281, 1242
$\nu_s(\text{C-O-C})$	1116	1112	1106	1105
$r(\text{CH}_2)$	960, 947, 844	962, 948, 844	963, 948, 844	963, 948, 843
$I_{1360}/I_{1467}(\text{H})$	0.857	0.794	0.732	0.733
$I_{1343}/I_{1467}(\text{T})$	0.286	1.29	1.43	1.66
$I_{1281}/I_{1467}(\text{H})$	1.29	1.03	0.795	0.914
$I_{1242}/I_{1467}(\text{T})$	0.310	0.647	0.798	0.820
$I_{948}/I_{1467}(\text{H})$	0.701	0.740	0.643	0.651
$I_{962}/I_{1467}(\text{T})$	0.211	1.07	1.19	1.36
$I_{844}/I_{1467}(\text{H})$	1.29	1.23	1.13	1.16

a: the subscript x of  $I_x$  represents other peak intensity

**Fig. 5** Fitting curves of FTIR traces at the region from  $1400\text{--}1320\text{ cm}^{-1}$  for all PEO films



$1467\text{ cm}^{-1}$  as reference because the peak intensity and position of  $1467\text{ cm}^{-1}$  are not affected by conformation and crystallinity of PEO [16–20].

To quantitatively analyze the peak intensity of specific bands corresponding to H or T structures, it becomes necessary to use Origin 8.6 to accurately fit the FTIR traces of PEO on the basis of Gaussian distribution, as shown in Fig. 5, for instance. The peak intensity ratios of H or T structure are given in Table 2. Table 2 can be read either along each row or down each column. From the first column, one can see that all the peak intensity ratios of H structure are much larger than those corresponding to T structure, implying that at low molecular weight, H structure is dominant in PEO chains as the H structure is more thermodynamically stable. With increasing the molecular weight, the peak intensity ratios of H structure drop slightly, on the contrary, those of T structure increase dramatically, as shown from column1 to column2, indicating that molecular weight has significantly affected the conformation of PEO chains. From column2 (PEO-10) to column4 (PEO-400), the increase in the peak intensity ratio for T structure becomes medium, which is different from that varies from column1 (PEO-0.5) to column2 (PEO-10). As we all know, the change in the conformation of molecular chain may be caused by applied external tension [12] and interactions within PEO matrix, like chemical or physical interactions [10, 12]. Which parameters will be responsible for the conformation changes in PEO films with molecular weight varied from  $5'000$  to  $4'000'000$ ? This will be discussed in detail later.

#### Crystallinity measurement of PEO membranes

The results from XRD (two sharp peaks neighboring  $2\theta = 20^\circ$ ) and FTIR (the indicator of triplet peak of  $\text{--C--O--C--}$  band [1]) measurements interpret that a crystalline structure has been formed in PEO films. In this section, we adopt the DSC testing to evaluate the deviations of crystallinity and melting temperature of PEO films under programs controlling temperature. The calculation of relative crystallinity of PEO has been expressed in Ref. [1] thoroughly, and results are interpreted in Fig. 6. Without respect of programs controlling temperature (in Fig. 6a), the crystallinity of PEO films decreases abruptly with increasing molecular weight, and no evident derivations in crystallinity can be observed in each PEO films. The decrease in crystallinity of PEO films with increasing molecular weight may be associated with the exclusion of some molecular chain segments outside the crystalline lamellae, like entanglements existed in certain amorphous solid state. In Fig. 6b, the melting temperature of PEO films evolves to higher temperature with increasing molecular weight, which is ascribed to molecular weight dependent and shifts to lower temperature as molecular weight decreases [21]. To our interest, the amplitude of variation in melting temperature of PEO-0.5 is much larger than those of the other three, which may be something different between PEO-0.5 and the other three. Xie et al. suggested that the derivation in melting temperature under repeated heating processes is an indicator of certain interactions occurring in PEO films, which depends on the molecular weight [22].



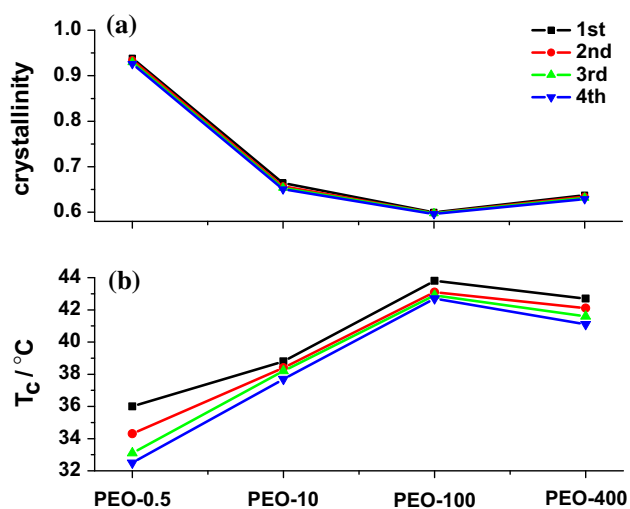


**Fig. 6** Variations of **a** crystallinity and **b** melting temperature of PEO films with different molecular weights

## Discussion

Due to the molecular flexibility of PEO (the energy difference between H and T structures is calculated to be only  $\sim 0.42$  kJ/mol [9]), which kind of conformations adopted by PEO films is dependent on the environment of PEO molecular chains. There is no doubt that two conformations will coexist in PEO films when casting from solutions [9]; however, the thermodynamically more stable H structure would be predominant because of little lower packing energy. The T structure takes predominant only by applying an external tension to PEO matrix [12], or by incorporating with some molecules, like water [12], PVC [23], syndiotactic, or atactic PMMA [9], or by preparing from the freeze-dried PEO/benzene dilute solution [11]. As we mention in the FTIR measurement, why do PEO molecular chains take preferentially a T structure in conformations with increasing molecular weight under our experiment?

In other researchers' previous works, Ramana [24] envisaged pairwise electrostatic interactions between positive and negative sites of PMMA and PEO. Due to the strong electrons withdrawing effect of oxygen atoms, the positive carbonyl carbon atom in PMMA acted as an electron acceptor, where lone pairs of electrons of the negative oxygen atoms in PEO had to act as an electron donor, which facilitated the H structure configuration to transform into the T structure. Marcos et al. adopted this view and further pointed out that two T structure PEO units may match three syndiotactic PMMA units on the base of the fact that the repeat distances of the syndiotactic PMMA structure and T structure of PEO are approximately 4.8 Å [9] and 7.12 Å [12], respectively. In this case, however, in the pure PEO films, the C atoms carried certain positive charge while the oxygen atoms possessed parts of negative

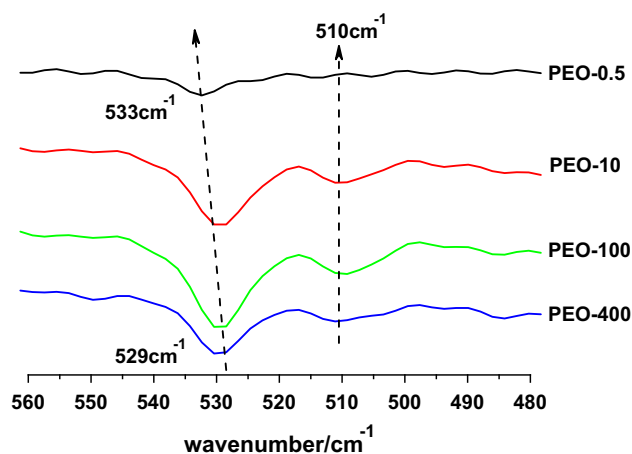


**Fig. 7** Traces of  $\text{-C-C-O-}$  bending regions of PEO films with different molecular weights

charge due to the stronger electronegativity of oxygen atom as compared to C atom; thus, the strength of electrostatic interaction between two PEO molecular chains would be independent of molecular weight. That is, without respect to molecular weight, the H structure and T structure will be constant in PEO films under the same preparing method, which disagrees with our experimental observations.

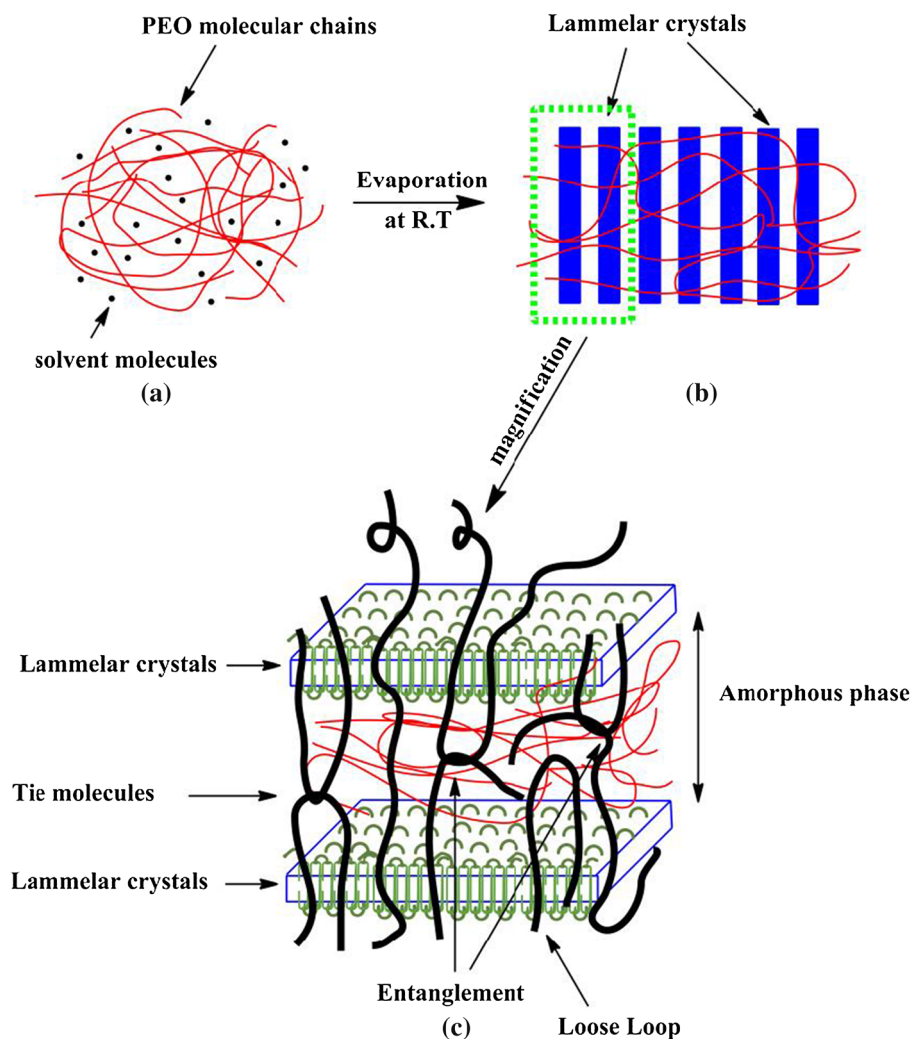
On the other hand, Gu et al. proposed that based on the fact that the trans planar chain conformation of PEO is rather stable at room temperature by preparing from freeze-dried approach, chain coils of PEO are more likely to suffer from the tension associated with the force of crystallization of solvent benzene [11]. The effect just equals to be a situation when an external stress is applied to the sample using a mechanic elongation device. Bergeron et al. reported that the FTIR traces of  $\text{-C-C-O-}$  bending region between 560 and 500  $\text{cm}^{-1}$  are very sensitive to tensions [13]. As shown in Fig. 7 from our experimental observation, only one evident and rather flat peak at 533  $\text{cm}^{-1}$  can be recognized in PEO-0.5, however, for the other three, two peaks, one at 529  $\text{cm}^{-1}$  and the other at 510  $\text{cm}^{-1}$ , emerge clearly, and the peak intensities become stronger. Meanwhile, a red shift of 4  $\text{cm}^{-1}$  has been recognized around the peak position of 529  $\text{cm}^{-1}$ , which is the indicator of internal tension/strain and orientation [13]. Combined displacements of peak position and peak intensities of  $\text{-CH}_2\text{-}$  and  $\text{-C-O-C-}$ , the peak intensity ratio of H and T structure (FTIR measurement), the XRD and DSC observations with Fig. 7, and the possible interactions of PEO molecular chains to explain the difference between H and T structure of PEO films with molecular weight are proposed in Fig. 8.

In Fig. 8a, PEO powders with different molecular weights are dissociated in the acetonitrile (the solute concentration of PEO is 9.54 wt%). Due to the linear flexible

structure of the PEO macromolecules, this polymer shows a particular ability to form entangled physical bonds [3], and then entanglement-enrich domains are formed within all solutions [13]. As the molecular weight increases, the rheological viscosity of solutions becomes much denser, and the content of entanglement-enrich domains increases. When the solution-casting films are evaporated at room temperature (R.T), some PEO molecular chains become order and participate in the formation of lamellar crystals, as illustrated in Fig. 8b. During this process, some topological structures, like entanglements [25], tie molecules, and loose loop [26] (as shown in Fig. 8c), do not participate into crystals as the time required for a disentangling depends on the local mobility [27]. That is, the time required for disentanglement is longer than the initial crystal growth time, especially for high molecular weight polymer films [21]. Thereby, crystallization does not necessitate the chain disentanglement and just occurs within the regions of “free” and order PEO molecular chains. As a result, the entanglements are excluded outside

the lamellar crystals and just shift into the amorphous regions, which accommodates themselves in the interlamellar space with some PEO molecular chains pass through certain regular lamellar crystals (Fig. 8b). With the order PEO molecular segments adjusting them into crystal cells, the lamellar crystals act as “solidification region” and freeze the crystal PEO segments, leading to the difference in the specific volume between crystal and amorphous phases. As a consequence, an internal stress arises from the entanglements and tie molecules neighboring the surface of lamellar crystals. This specific intermolecular interactions should occur to force the molecule to flatten into a trans planar structure (T structure) [9], leading to the changes [17] in the peak intensity ratio of H or T structure and the displacement of peak positions of  $\nu_s(\text{CH}_2)$  to higher number and of  $\beta(-\text{C}-\text{C}-\text{O}-)$  or  $\nu_s(-\text{C}-\text{O}-\text{C}-)$  to lower number obtained from the FTIR spectra. With increasing the molecular weight of PEO, entanglements and tie molecules increase evidently [28–30]. And consequently, much more T structure emerges. However, this internal stress is

**Fig. 8** Scheme of entanglements and tie molecules in crystalline PEO





very weak, maybe only affects 1~2 repeat units of PEO segments (an approximate repeat distance T structure is about 7.12 Å [9]), which is much lower than that of PEO chains under tension or freeze-dried approach. Thereby, in the case of tension or freeze-dried approach, an obvious peak at about  $2\theta = 25^\circ$  of PEO films is observed, which is the indicator of long-range order of PEO chains (trans planar zigzag crystal) [12]. But no peak at  $2\theta = 25^\circ$  can be seen in PEO films prepared by drying and crystallizing at room temperature, indicating that only a short-range order (T structure) of the PEO molecular segments is introduced by entanglements and tie molecules, which cannot be detected by XRD, as shown in Fig. 2.

## Conclusions

The conformation of PEO films, prepared from solution-casting method, with different molecular weights is investigated by XRD, FTIR, and DSC measurements exhaustively. The XRD profiles show two crystalline peaks, one at about  $2\theta = 19^\circ$  and another at about  $2\theta = 23^\circ$ . Calculation from XRD parameters supports the fact that the crystal lattice of PEO films adopts the monoclinic crystal structure, without respect to molecular weight. The crystallinity decreases from 93.82 to 59.62 % with increasing molecular weight, and the deviation of crystallinity of each PEO films can be ignored under four reheated cycles. However, the crystalline temperature shifts to lower temperature as molecular weight decreases, indicating such a change is molecular weight dependent. Meanwhile, the deviation of crystalline temperature of PEO-0.5 is larger than those of the other three under four reheated cycles. From FTIR traces, the peak intensity ratio of helix structure (H structure), the most characteristic bands of which are at 1360 ( $-\text{CH}_2-$  wagging), 1281 ( $-\text{CH}_2-$  twisting), 948, and 843  $\text{cm}^{-1}$  ( $-\text{CH}_2-$  rocking), decreases with increasing molecular weight. In contrast, trans planar structure (T structure), the most characteristic bands of which locate at 1343 ( $-\text{CH}_2-$  wagging), 1242 ( $-\text{CH}_2-$  twisting), and 962  $\text{cm}^{-1}$  ( $-\text{CH}_2-$  rocking), increases dramatically. Furthermore, stretching vibrations of  $-\text{CH}_2-$  have changed with molecular weight, illustrating that the circumstance of  $-\text{CH}_2-$  is different. A red shift about 11  $\text{cm}^{-1}$  is observed in the stretching vibration of  $-\text{C}-\text{O}-\text{C}-$  with increasing molecular weight, suggesting that some interactions may be introduced. Simultaneously, the  $-\text{C}-\text{C}-\text{O}-$  bending region sensitive to tensions between 560 and 500  $\text{cm}^{-1}$  shifts to lower wavenumber, and a new peak at about 510  $\text{cm}^{-1}$  emerges, which is the indicator of internal tension/strain and orientation.

Consequently, with respect to the molecular weight, the possible interactions of PEO molecular chains to explain

the difference between H and T structure of PEO films are proposed. When casting from PEO solution, entanglement-enrich domains will be dominant. After evaporation at room temperature, the lamellar crystals act as “solidification region” and freeze the crystal PEO segments by adjusting the order PEO molecular segments into crystal cells. As a result, an internal stress arises from the entanglements and tie molecules neighboring the surface of lamellar crystals and occurs to force the molecule to flatten into a trans planar structure (T structure), which is in accordance with our experimental observation quite well.

**Acknowledgements** The authors gratefully acknowledge the financial support from The National Natural Science Funds of China (No.51303026) and the foundation of Chemical Industrial Cleaner Production and Green Chemical R&D Center of Guang Dong Universities (201401).

## References

1. Yang S, Liu Z, Jiao Y et al (2013) Study on the compatibility and crystalline morphology of NBR/PEO binary blends. *J Mater Sci* 48:6811–6817. doi:10.1007/s10853-013-7486-3
2. Zhang G, Jin L, Zheng P et al (2013) Molecular weight dependence of crystal pattern transitions of poly(ethylene oxide). *Chin J Polym Sci* 31:798–808
3. Apicella A, Cappello B, Del Nobile M et al (1993) Poly(Ethylene oxide) (PEO) and different molecular weight PEO blends monolithic devices for drug release. *Biomaterials* 14:83–90
4. Luo W, Liu Y, Yang S et al (2014) Synthesis and conduction mechanism of comb-like Polymethacrylate solid polymer electrolytes. *Acta Polym Sin* 45:63–71
5. MacGlashan G, Andreev Y, Bruce P (1999) Structure of the polymer electrolyte poly(ethylene oxide)<sub>6</sub>:LiAsF<sub>6</sub>. *Nature* 398:792–794
6. Yang S, Liu Z, Jiao Y et al (2014) New insight into PEO modified inner surface of HNTs and its nano-confinement within nanotube. *J Mater Sci* 49:4270–4278. doi:10.1007/s10853-014-8122-6
7. Stoeva Z, Martin-Litas I, Staunton E et al (2003) Ionic Conductivity in the crystalline polymer electrolytes PEO<sub>6</sub>:LiXF<sub>6</sub>, X = P, As, Sb. *J Am Chem Soc* 125:4619–4626
8. Andreev Y, Bruce P (2000) Polymer electrolyte structure and its implications. *Electrochim Acta* 45:1417–1423
9. Marcos J, Orlandi E, Zerbi G (1990) Poly(ethylene oxide)-poly(methyl methacrylate) interactions in polymer blends: an infra-red study. *Polymer* 31:1899–1903
10. Takahashi Y, Tadokoro H (1973) Structural studies of polyethers,  $-(\text{CH}_2)_m\text{O}-\text{n}$ . X. Crystal structure of poly(ethylene oxide). *Macromolecules* 6:672–675
11. Gu F, Bu H, Zhang Z (2000) A unique morphology of freeze-dried poly(ethylene oxide) and its transformation. *Polymer* 41:7605–7609
12. Takahashi Y, Sumita I, Tadokoro H (1973) Structural studies of polyethers. IX. Planar zigzag modification of poly(ethylene oxide). *J Polym Sci Polym Phys Ed* 11:2113–2122
13. Bergeron C, Perrier E, Potier A et al (2012) A study of the deformation, Network, and aging of polyethylene oxide films by infrared spectroscopy and calorimetric measurements. *Int J Spectrosc* 2012:1–13
14. Jurkin T, Pucić I (2013) Irradiation effects in poly(ethylene oxide)/silica nanocomposite films and gels. *Polym Eng Sci* 53:2318–2327

15. Frech R, Huang W (1995) Conformational changes in diethylene glycol dimethyl ether and poly(ethylene oxide) induced by lithium ion complexation. *Macromolecules* 28: 1246–1251
16. Xu J, Xiong Q, Liang G et al (2009) Ion-polymer interactions in  $\text{SmCl}_3(\text{H}_2\text{O})_6$  doped poly(ethylene oxide) electrolytes. *J Macromol Sci B* 48:856–866
17. Liang G, Xu J, Xu W et al (2011) Effect of filler-polymer interactions on the crystalline morphology of PEO-based solid polymer electrolytes by  $\text{Y}_2\text{O}_3$  nano-fillers. *Polym Compos* 32:511–518
18. Everall N, MacKerron D, Winter D (2002) Characterisation of biaxial orientation gradients in poly(ethylene terephthalate) films and bottles using polarised attenuated total reflection FTIR spectroscopy. *Polymer* 43:4217–4223
19. Kher A, Udabage P, McKinnon I et al (2007) FTIR investigation of spray-dried milk protein concentrate powders. *Vib Spectrosc* 44:375–381
20. Cheng H, Zhu C, Yang Y (2007) FTIR characterization of ion association and phase composition in PEO-based polymer electrolytes. *Acta Chim Sin* 65:2832–2838
21. Fu Q, Strobl G (2002) Role and importance of radius of gyration of chains in the melt in the crystallization of poly(1-butene). *Chin J Polym Sci* 20:143–154
22. Chen N, Xie X (2013) Confined crystallization of poly(ethylene oxide) under copper(II) ion coordination-defect-induced melting point depression. *Acta Polym Sin* 44:635–642
23. Marentette J, Brown G (1998) The crystallization of poly(ethylene oxide) in blends with neat and plasticized poly(vinyl chloride). *Polymer* 39:1415–1427
24. Rao G, Castiglioni C, Gussoni M et al (1985) Probing the structure of polymer blends by vibrational spectroscopy: the case of poly(ethylene oxide) and poly(methyl methacrylate) blends. *Polymer* 26:811–820
25. Yang S, Liu L, Jia Z et al (2014) Study on the structure-properties relationship of natural rubber/ $\text{SiO}_2$  composites modified by a novel multi-functional rubber agent. *Express Polym Lett* 8:425–435
26. Humbert S, Lame O, Vigier G (2009) Polyethylene yielding behaviour: what is behind the correlation between yield stress and crystallinity? *Polymer* 50:3755–3761
27. Fu Q, Heck B, Strobl G et al (2001) A temperature- and molar mass-dependent change in the crystallization mechanism of Poly(1-butene): transition from chain-folded to chain-extended crystallization? *Macromolecules* 34:2502–2511
28. Pandey A, Champouret Y, Rastogi S (2011) Heterogeneity in the distribution of entanglement density during polymerization in disentangled ultrahigh molecular weight polyethylene. *Macromolecules* 44:4952–4960
29. Pandey Y, Papakonstantopoulos G, Doxastakis M (2013) Polymer/Nanoparticle interactions: bridging the gap. *Macromolecules* 46:5097–5106
30. Pandey A, Toda A, Rastogi S (2011) Influence of amorphous component on melting of semicrystalline polymers. *Macromolecules* 44:8042–8055